International Journal of Engineering Research & Technology (IJERT)
ISSN: 2278-0181
Vol. 14 Issue 12 , December - 2025

Analysis of Cracks in Rigid and Flexible Pavements on Road Failures using Crack Investigation Mechanism

Egbebike, M.O.
Department of Civil Engineering, Nnamdi Azikiwe University, Awka, Nigeria;
and Shell Center of Excellence for Environmental Management and Green Energy,
University of Nigeria, Nsukka, Enugu Campus, Nigeria.
Ezeagu, C. A.
Department of Civil Engineering, Nnamdi Azikiwe University, Awka, Nigeria.
Ibeabuchi C.I.
Department of Civil Engineering, Nnamdi Azikiwe University, Awka, Nigeria.

Abstract - Pavement cracking is a major factor contributing to road failures, affecting both rigid and flexible pavement structures. This study investigates the initiation and propagation of cracks in these pavement types using finite element modeling (FEM) techniques. Rigid pavements, modeled as concrete slabs on an elastic foundation, were analyzed for crack formation at slab edges and joints, while flexible pavements were simulated as multi-layered asphalt structures to evaluate top-down and bottom-up cracking mechanisms. The FEM simulations, conducted using STAAD Pro, incorporated material properties, stress distribution, and load conditions derived from empirical studies. Results indicate that rigid pavements are prone to fatigue and shrinkage-induced cracking, whereas flexible pavements primarily experience surface-initiated cracks due to repeated loading. The findings were validated against field data, highlighting the influence of pavement thickness, subgrade stiffness, and material strength on crack development. This research provides insights for improving pavement design and maintenance strategies, ultimately enhancing roadway durability.

Keywords: Pavement cracking, Rigid pavements, Flexible pavements, Finite element modeling, Crack propagation, STAAD Pro

1. INTRODUCTION

Pavement infrastructure is essential for transportation networks, serving as the foundation for efficient vehicular movement and economic development. However, pavement deterioration, particularly cracking, remains a significant challenge globally, especially in developing countries. Cracking in pavements compromises structural integrity, shortens service life, and escalates maintenance costs. The ability to understand and model crack initiation and progression is therefore vital for sustainable pavement engineering.

In Nigeria and many parts of sub-Saharan Africa, road failures are increasingly attributed to poor pavement design, insufficient maintenance, substandard materials, and environmental conditions. A proper investigation into the mechanical and structural behavior of pavement types (rigid and flexible) is necessary to propose effective engineering solutions. This study uses a crack investigation mechanism anchored on finite element modeling (FEM) and empirical observations to analyze cracking patterns in pavements.

2. LITERATURE REVIEW

2.1 Crack Formation in Rigid Pavements

Rigid pavements, primarily constructed with Portland Cement Concrete (PCC), are susceptible to cracking due to shrinkage, thermal stresses, and fatigue loading. Shrinkage cracking typically results from volumetric changes during curing. [1] identified fracture toughness as a critical parameter in understanding these failure mechanisms. Temperature-induced expansion and contraction also lead to longitudinal and transverse cracking [2]. Fatigue cracking often occurs at joints and slab edges due to repeated traffic loads. Studies such as [3] have demonstrated that fracture mechanics models, both linear elastic (LEFM) and

International Journal of Engineering Research & Technology (IJERT)
ISSN: 2278-0181
Vol. 14 Issue 12 , December - 2025

nonlinear (NLFM), are suitable for analyzing crack propagation in rigid pavements. The influence of slab thickness, joint spacing, and subgrade stiffness on crack development has also been highlighted [4]

2.2 Crack Formation in Flexible Pavements

Flexible pavements comprise multiple layers, including asphalt concrete, base, and subgrade. Two dominant cracking mechanisms exist: top-down and bottom-up cracking. Top-down cracks begin at the surface due to tensile stress from traffic loads, exacerbated by asphalt binder aging [5][6]. Bottom-up cracks initiate from the lower asphalt layers under tensile stresses and propagate upward, especially where the pavement is thin or the subgrade is weak [7].
Environmental impacts such as moisture and temperature variations play a crucial role in accelerating crack propagation. Proper modeling of these phenomena is essential for effective pavement management strategies [8].

2.3 Finite Element Modeling in Pavement Crack Analysis

FEM has gained prominence in pavement design due to its capability to simulate stress distributions and crack behavior under realistic loading and boundary conditions. [2] emphasized FEM's utility in analyzing complex pavement responses. In flexible pavements, cohesive zone models and damage mechanics are widely used [6]. For rigid pavements, FEM incorporates crack modeling using stress intensity factors and Winkler-type elastic foundations [3].
This study adopts FEM to evaluate crack behavior in pavement systems under various conditions, integrating theoretical modeling with real-world field data for validation.

3. METHODOLOGY

3.1 Finite Element Modeling Approach

A finite element modeling (FEM) approach was employed using STAAD Pro software to analyze crack initiation and propagation in rigid and flexible pavements. FEM enables detailed simulation of pavement stress distribution, deformation, and crack development under various loading conditions [2].

3.1.1 Model Description

Rigid Pavement: Modeled as a concrete slab on an elastic foundation (Winkler model) to simulate subgrade support. The slab dimensions and material properties were based on standard highway pavement structures [3].

Flexible Pavement: Simulated as a multi-layered system comprising an asphalt concrete layer, base, and subgrade. The asphalt layer was assigned viscoelastic properties to capture realistic pavement behavior under loading [6].

3.1.2 Material Properties and Boundary Conditions

To accurately model the structural response of rigid and flexible pavements under loading, appropriate material properties were assigned to each layer within the finite element simulation. Material properties were selected based on empirical studies and pavement design standards [1][7]. The key parameters are presented in Table 1.

Table 1. Key Parameters

Material	Elastic Modulus (MPa)	Poisson's Ratio	Tensile Strength (MPa)	Compressive Strength (MPa)
Concrete (Rigid Pavement)	30,000	0.2	3.5	40
Asphalt (Flexible Pavment)	5,000	0.35	2.0	10
Subgrade	100	0.4	N/A	N/A

International Journal of Engineering Research & Technology (IJERT)
ISSN: 2278-0181
Vol. 14 Issue 12 , December - 2025

Boundary conditions were applied to simulate real-world pavement loading scenarios. The bottom of the subgrade was fixed, while vertical loads were applied to represent vehicular tire pressure [8].

3.1.3 Crack Modeling and Analysis

Rigid Pavement: Crack propagation was analyzed using fracture mechanics principles, considering stress intensity factors at slab edges and joints [2][3]. Flexible Pavement: The cohesive zone model was employed to simulate top-down cracking, tracking crack initiation at the surface and its progression under repeated loading [6][9].

Crack modelling equation for flexible and rigid pavement.

The Griffith Fracture criterion, one of the most widely accepted theory of fracture mechanics of concrete with its governing law for crack propagation is based on the inelastic materials behavior using the theory of Linear Elastic Fracture Mechanics (LEFM) and Non Linear Fracture Mechanics (NLFM). He presented two (2) major computation theories in crack analysis of concrete which can be extended to crack analysis of flexible pavement namely: Discrete Crack Modelling Approach and Smeared Crack Modelling Approach. Fundamental concept of Linear Elastic Mechanics is based on the crack forms observed in both rigid and flexible pavement on site

Figure 1 illustrates the geometric representation of a typical cracked pavement section as used in the finite element modeling. The figure shows a schematic crack tip and propagation zone in both rigid and flexible pavements, using a polar coordinate system (r, θ) around the crack tip. This configuration supports the application of Linear Elastic Fracture Mechanics (LEFM) and Nonlinear Fracture Mechanics (NLFM) principles in analyzing crack behavior under repeated loading conditions.

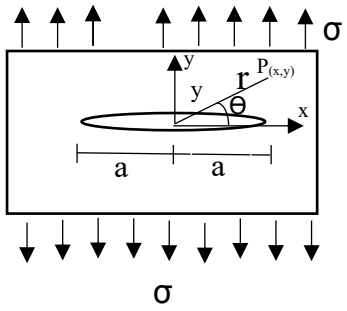

Fig 1. Typical failed pavement section

For a near – tip point P(x,y)

$X = a + rcos\theta$ eqn. 1

$Y = y + rsin\theta$ eqn. 2

Where X = crack length (horizontal length of crack)

Y = crack depth (vertical depth of crack)

a) Finite Element Modelling

The rigid pavement was modelled on Staad Pro software as plates on elastic foundation. Figure 2 presents the finite element model (FEM) of a pavement plate structure used for simulating the structural response of rigid and flexible pavements. The model represents the pavement as a series of interconnected plate elements laid over an elastic foundation (Winkler-type springs) that simulate subgrade support. For rigid pavement, concrete plates were modeled with varying thicknesses, while flexible pavement

International Journal of Engineering Research & Technology (IJERT)
ISSN: 2278-0181
Vol. 14 Issue 12 , December - 2025

layers were assigned viscoelastic properties. This mesh configuration allowed for detailed analysis of deflection, bending, torsional behavior, and crack initiation across a range of loading scenarios.

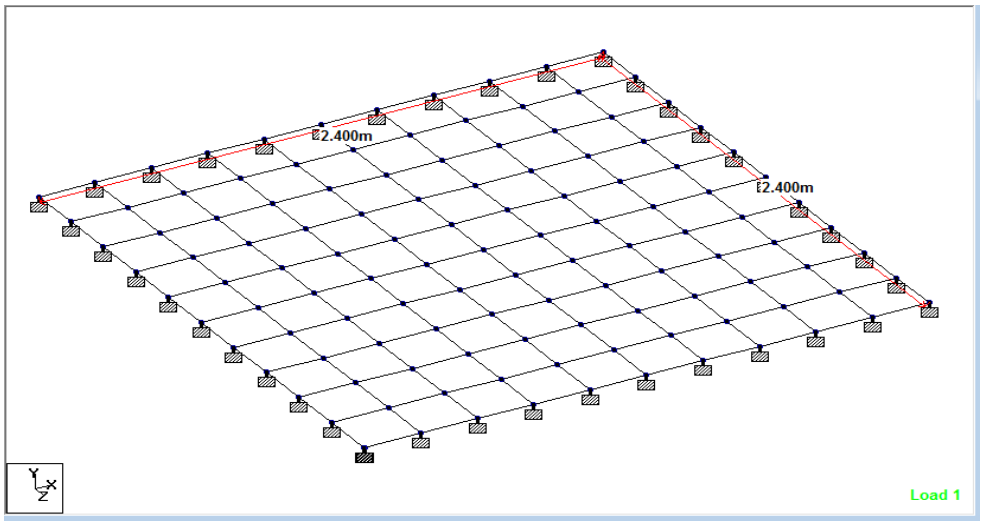

Figure 2: Pavement Plate model

Plate Models were generated for 2 materials: concrete and bitumen/asphalt. Each material was modeled at different thicknesses ranging from 25mm to 300mm at increments of 25mm. The maximum deflection, Bending Moment, Torsion and shear stress for each model were determined to evaluate the characteristic nature of each material under the specified loading.

These models were generated by data gotten through field and laboratory investigation which included the following

(i) Distress Survey and Non-destructive assessment on 3 Flexible and 3 Rigid pavement sections at three different locations namely: Awka in Anambra Central zone (INEC road Okpuno, Amawbia Junction, Amawbia-Nawgu-Ukwulu –Igbariam road), Onitsha in Anambra North zone (Holy Trinity/33 road/CPS roads, Federal Government Secondary School Onitsha 3-3 internal roads) and Nnewi in Anambra South zone (Oba Nnewi old road, Oba Nnewi new road).

(ii) Experimental study on the cored samples tested at Anambra State Material Testing Laboratory to determine the following: Marshall Stability & Flow, Extraction of Bitumen and Bulk Density and void on the pavements.

b) Load Analysis

Westergaard's theory which considered three critical locations of the wheel load on the pavement was used for the loading of the models. This is defined by the 3 load cases stated below:

Case 1: Load is applied at the corner of a rectangular slab. This provides for the cases when the wheel load is applied at the intersection of the pavement edge and a transverse joint.

Case 2: Load is applied at the interior of the slab at a considerable distance from its edges.

Case 3: Load is applied at the edge of the slab at a considerable distance away from any corner.

The following parameters were used for the load analysis of the models

Applied the maximum HA loading = 80 tonnes = 80,000 kg = 784.8 kN

Total area of plate = 2.4 x 2.4 m = 5.76 m^2

Equivalent uniformly distributed load on plate = $\frac{784.8}{5.76}$ = 136.25 kN/m^2

International Journal of Engineering Research & Technology (IJERT)
ISSN: 2278-0181
Vol. 14 Issue 12 , December - 2025

3.1.4 Validation of Numerical Results

To validate the FEM simulations, numerical results were compared with field data from past studies on pavement distress in Nigeria [10][11]. Stress distributions, crack propagation patterns, and failure modes were analyzed to ensure consistency with observed pavement deterioration.

4. RESULTS AND DISCUSSION

4.1 Analysis of Results

4.1.1 Material 1 – Concrete

Table 2 presents the results of the FEM simulation showing how deflection in rigid (concrete) pavements varies with slab thickness. Pavement thicknesses ranged from 25 mm to 300 mm in 25 mm increments. The table also includes corresponding values for bending moments, torsional moments, and shear stress. The data illustrate the significant reduction in deflection as concrete slab thickness increases, confirming improved structural rigidity and load-bearing capacity.

Modulus of Elasticity = 2.17 x 10^7kN/m^2 Poisson ratio = 0.2

Table 2: Variation of deflection with plate thickness (concrete)

Thickness (mm)	Deflection (mm)	Bending Moment (kNm/m)		Torsion (kNm/m)	Shear Stress (N/mm^2)
		Hogging	Sagging		
25	192.788	24.925	15.809	7.159	4.748
50	24.22	24.938	15.820	7.115	2.372
75	7.237	24.950	15.835	7.045	1.578
100	3.088	24.954	15.954	6.956	1.18
125	1.603	24.945	15.876	6.854	0.941
150	0.943	24.923	15.900	6.744	0.781
175	0.605	24.886	15.925	6.631	0.666
200	0.414	24.835	15.951	6.518	0.580
225	0.298	24.886	15.925	6.409	0.512
250	0.222	24.711	16.006	6.304	0.458
275	0.172	24.636	16.033	6.206	0.414
300	0.136	24.555	16.060	6.114	0.377

4.1.2 Material 2 – Bitumen/Asphalt

Table 3 shows the deflection and associated stress responses for flexible (asphalt) pavements under the same loading conditions and thickness ranges as the concrete model. Due to the lower modulus of elasticity of asphalt, deflections are significantly higher at thinner layers. The table includes bending and torsional moment values along with shear stresses, highlighting the material's viscoelastic behavior under load.

Modulus of Elasticity E = 4.89 x 10^5 kN/m^2 Poisson's ratio = 0.25

International Journal of Engineering Research & Technology (IJERT)
ISSN: 2278-0181
Vol. 14 Issue 12 , December - 2025

Table 3: Variation of deflection with plate thickness (Bitumen/Asphalt)

Thickness (mm)	Deflection (mm)	Bending Moment (kNm/m)		Torsion (kNm/m)	Shear Stress (N/mm^2)
		Hogging	Sagging		
25	8365.526	24.879	16.468	6.714	4.745
50	1051.242	24.891	16.479	6.670	2.370
75	314.298	24.902	16.496	6.601	1.577
100	134.187	24.903	16.517	6.513	1.180
125	69.729	24.889	16.541	6.412	0.940
150	41.063	24.861	16.567	6.303	0.780
175	26.38	24.817	16.595	6.191	0.665
200	18.069	24.761	16.624	6.079	0.579
225	13.003	24.693	16.653	5.971	0.512
250	9.731	24.616	16.683	5.868	0.458
275	7.518	24.533	16.712	5.771	0.413
300	5.964	24.444	16.742	5.681	0.376

Figure 3 displays the transverse bending moment distribution for Load Case 1, where the wheel load is applied at the corner of the pavement slab. The high concentration of negative (hogging) and positive (sagging) bending moments near the corners indicates the critical stress zones where cracking is most likely to initiate. This supports the numerical results from Table 4 showing maximum settlement and base pressure in this region.

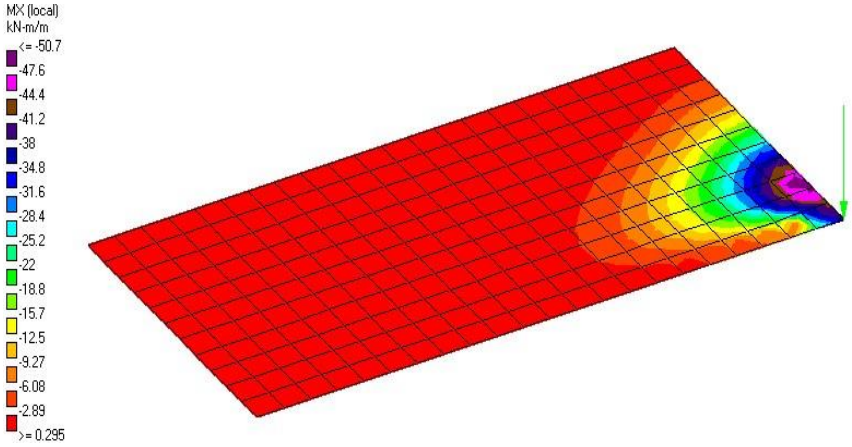

Figure 3: Typical transverse bending moment diagram when the wheel load is at the corner.

International Journal of Engineering Research & Technology (IJERT)
ISSN: 2278-0181
Vol. 14 Issue 12 , December - 2025

Figure 4 presents the transverse bending moment profile under Load Case 2, representing a centrally applied wheel load on the pavement slab. Compared to edge and corner loading, this configuration shows a more uniform moment distribution, with lower peak stresses, which correlates with lower crack initiation risk. The figure confirms the numerical trends from Table 5 regarding internal load stability in thicker pavements.

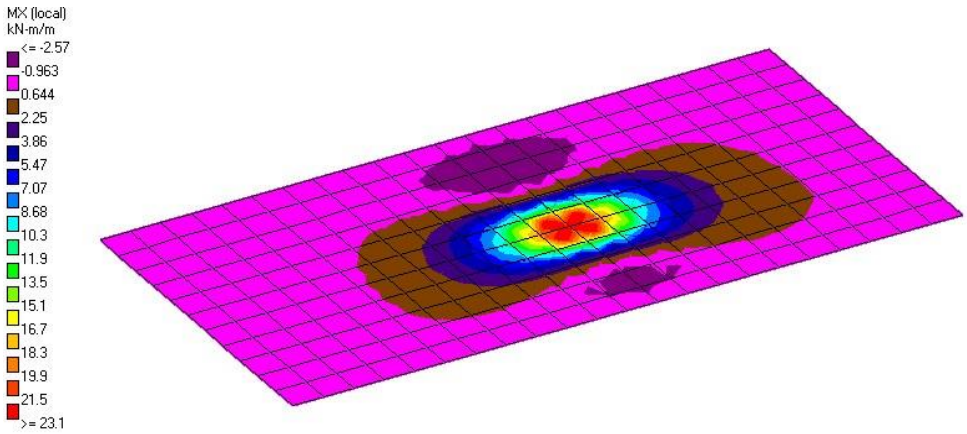

Figure 4: Typical transverse bending moment diagram when the wheel load is at the centre

Figure 5 illustrates the transverse bending moment distribution for Load Case 3, where the wheel load is applied at the edge of the pavement slab. The diagram reveals asymmetric moment profiles with pronounced gradients along the slab perimeter, highlighting elevated stress concentrations at slab boundaries. These regions are especially prone to tensile cracking due to reduced lateral support, aligning with results shown in Table 6.

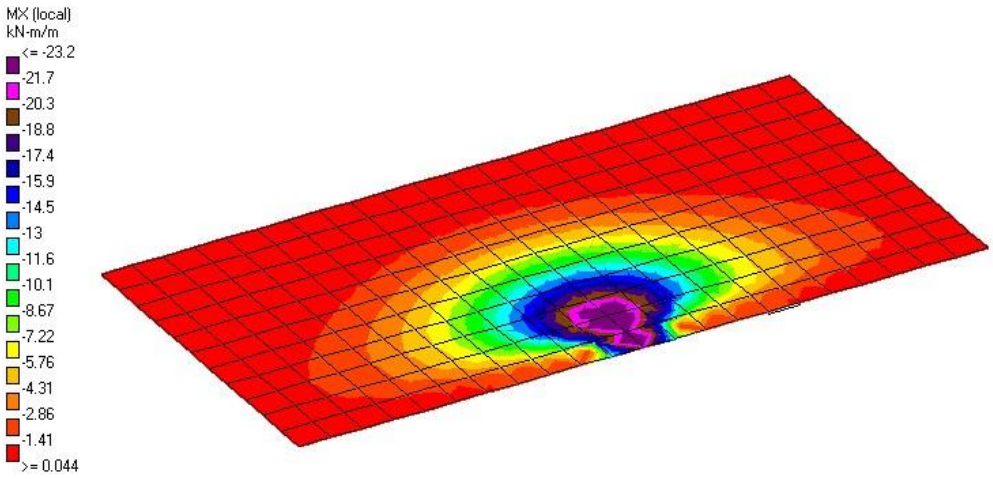

Figure 5: Typical transverse bending moment diagram when the wheel load is at the edge

To simulate stress concentration and deformation patterns in rigid pavement, a finite element analysis was conducted for Load Case 1, in which a wheel load is applied at the corner of a rectangular slab. This load condition replicates a critical failure scenario where tensile stresses are expected to peak due to minimal structural support at the intersection of pavement edges and joints. Table 4 presents the numerical results for different values of subgrade reaction modulus (k), showing variations in bending moments (Mx, My), torsional moment (Mxy), shear forces (Qx, Qy), maximum settlement, and base pressure for a slab thickness of 100 mm.

International Journal of Engineering Research & Technology (IJERT)
ISSN: 2278-0181
Vol. 14 Issue 12 , December - 2025

Table 4: Load Case 1: Wheel load at the corner for pavement thickness of 100mm

Modulus of subgrade reaction (kN/m²/m)	M_x (kNm/m)	M_y (kNm/m)	M_{xy} (kNm/m)	Q_x (N/mm²)	Q_y (N/mm²)	Maximum settlement (mm)	Base Pressure (kN/m²)
10,000	53.161	53.186	73.505	3.697	3.698	47.452	474.515
50,000	44.851	44.856	64.1348	3.379	3.379	20.882	1044.09
75,000	43.036	43.038	61.090	3.249	3.249	16.909	1268.21
100,000	41.383	41.384	58.725	3.143	3.142	14.533	1453.34
200,000	36.192	36.192	52.257	2.828	2.828	10.009	2001.810

Thickness of pavement = 100 mm; E = 3.3 x 10^7 kN/m²; Poisson ratio = 0.2; f_{ck} = 30 N/mm²; f_{ctm} = 2.9 N/mm²

In Load Case 2, the wheel load is applied at the interior of the concrete slab, representing a more uniformly supported region of the pavement system. This configuration typically yields lower tensile stress levels compared to edge or corner loading scenarios. The analysis provides insight into pavement behavior under typical mid-lane loading conditions. Table 5 summarizes the computed structural response metrics-including bending moments, torsional moment, shear forces, maximum deflection, and base pressure-across a range of subgrade stiffness values for the same 100 mm slab thickness.

Table 5: Load Case 2: Wheel load at the interior for pavement thickness of 100mm

Modulus of subgrade reaction (kN/m²/m)	M_x (kNm/m)	M_y (kNm/m)	M_{xy} (kNm/m)	Q_x (N/mm²)	Q_y (N/mm²)	Maximum settlement (mm)	Base Pressure (kN/m²)
10,000	25.746	25.725	5.7836	1.205	1.205	5.052	50.520
50,000	18.127	18.0855	4.790	1.1597	1.1591	2.197	109.849
75,000	16.303	16.294	4.485	1.1408	1.1400	1.788	134.070
100,000	15.056	15.060	4.294	1.121	1.124	1.564	154.590
200,000	12.216	12.224	3.625	1.075	1.075	1.093	218.60

Thickness of pavement = 100 mm; E = 3.3 x 10^7 kN/m²; Poisson ratio = 0.2; f_{ck} = 30 N/mm²; f_{ctm} = 2.9 N/mm²

Table 6 presents the structural response when the wheel load is applied at the edge of the slab (Load Case 3) for a 100 mm thick concrete pavement. This loading condition simulates scenarios where partial slab support leads to stress gradients near the slab perimeter. The table outlines how varying subgrade modulus values influence bending and torsional moments, shear forces, settlement, and base pressure under this edge loading condition.

International Journal of Engineering Research & Technology (IJERT)
ISSN: 2278-0181
Vol. 14 Issue 12 , December - 2025

Table 6: Load Case 3: Wheel load at the edge for pavement thickness of 100mm

Modulus of subgrade reaction ($kN/m^2/m$)	M_x (kNm/m)	M_y (kNm/m)	M_{xy} (kNm/m)	Q_x (N/mm^2)	Q_y (N/mm^2)	Maximum settlement (mm)	Base Pressure (kN/m^2)
10,000	24.117	50.782	22.296	1.639	2.612	17.167	171.67
50,000	21.186	33.854	18.558	0.1244	2.4322	7.660	383.00
75,000	20.159	29.854	17.905	1.486	2.364	6.244	468.27
100,000	19.634	27.109	17.387	1.447	2.3081	5.396	539.61
200,000	18.073	20.875	15.921	1.328	2.142	3.782	756.300

Thickness of pavement = 100 mm; E = 3.3 x 10^7 kN/m^2; Poisson ratio = 0.2; f_{ck} = 30 N/mm^2; f_{ctm} = 2.9 N/mm^2

Table 7 provides results for Load Case 1-wheel load at the corner-for an increased slab thickness of 150 mm. This configuration helps assess the role of additional thickness in mitigating tensile stresses and deformation at slab corners under corner loading conditions.

Table 7: Load Case 1: Wheel load at the corner for pavement thickness of 150mm

Modulus of subgrade reaction ($kN/m^2/m$)	M_x(kNm/m)	M_y(kNm/m)	M_{xy} (kNm/m)	Q_x (N/mm^2)	Q_y(N/mm^2)	Maximum settlement (mm)	Base Pressure (kN/m^2)
10,000	54.775	55.724	77.171	2.582	2.587	26.380	263.796
50,000	51.292	51.318	70.449	2.472	2.472	11.640	581.90
75,000	48.684	48.703	68.264	2.423	2.423	9.485	711.39
100,000	47.069	47.072	66.569	2.382	2.382	8.198	819.76
200,000	44.697	44.700	61.903	2.253	2.253	5.749	1149.8

Thickness of pavement = 150 mm; E = 3.3 x 10^7 kN/m^2;Poisson ratio = 0.2; f_{ck} = 30 N/mm^2; f_{ctm} = 2.9 N/mm^2

Table 8 details the pavement performance under Load Case 2-interior loading-at a slab thickness of 150 mm. It demonstrates the response of the system under central slab loading and how subgrade stiffness influences mechanical behavior.

International Journal of Engineering Research & Technology (IJERT)
ISSN: 2278-0181
Vol. 14 Issue 12 , December - 2025

Table 8: Load Case 2: Wheel load at the interior for pavement thickness of 150mm

Modulus of subgrade reaction ($kN/m^2/m$)	M_x(kNm/m)	M_y(kNm/m)	M_{xy} (kNm/m)	Q_x (N/mm^2)	Q_y(N/mm^2)	Maximum settlement (mm)	Base Pressure (kN/m^2)
10,000	30.561	32.365	6.094	0.8077	0.8121	2.972	29.718
50,000	23.922	23.786	5.528	0.7877	0.793	1.242	62.110
75,000	21.965	21.831	5.316	0.785	0.785	1.010	75.780
100,000	20.575	20.471	5.145	0.7745	0.7793	0.874	87.36
200,000	17.324	17.296	4.667	0.761	0.761	0.618	123.515

Thickness of pavement = 150 mm; E = 3.3 x 10^7 kN/m^2;Poisson ratio = 0.2; f_{ck} = 30 N/mm^2; f_{ctm} = 2.9 N/mm^2

Table 9 shows the mechanical response under Load Case 3-edge loading-for a slab thickness of 150 mm. This allows comparison of how edge-induced stress conditions evolve with increasing pavement thickness.

Table 9: Load Case 3: Wheel load at the edge for pavement thickness of 150mm

Modulus of subgrade reaction ($kN/m^2/m$)	M_x(kNm/m)	M_y(kNm/m)	M_{xy} (kNm/m)	Q_x (N/mm^2)	Q_y(N/mm^2)	Maximum settlement (mm)	Base Pressure (kN/m^2)
10,000	26.071	64.0551	24.1835	1.1136	1.7970	9.654	96.54
50,000	23.574	46.236	20.819	1.0820	1.725	4.234	211.700
75,000	23.121	41.913	19.719	1.067	1.697	3.464	259.70
100,000	22.687	38.889	19.368	1.052	1.674	3.004	300.382
200,000	21.203	31.827	18.369	1.007	1.606	2.130	425.942

Thickness of pavement = 150 mm; E = 3.3 x 10^7 kN/m^2;Poisson ratio = 0.2; f_{ck} = 30 N/mm^2; f_{ctm} = 2.9 N/mm^2

Table 10 presents structural performance results for Load Case 1-corner loading-at a slab thickness of 200 mm. This scenario provides insights into stress reduction benefits associated with further increases in slab thickness.

International Journal of Engineering Research & Technology (IJERT)
ISSN: 2278-0181
Vol. 14 Issue 12 , December - 2025

Table 10: Load Case 1: Wheel load at the corner for pavement thickness of 200mm

Modulus of subgrade reaction ($kN/m^2/m$)	M_x(kNm/m)	M_y(kNm/m)	M_{xy} (kNm/m)	Q_x (N/mm^2)	Q_y(N/mm^2)	Maximum settlement (mm)	Base Pressure (kN/m^2)
10,000	54.3816	58.4516	78.0866	1.9939	2.00308	17.771	177.77
50,000	54.617	54.8578	72.9006	1.9465	1.94725	7.668	383.408
75,000	53.541	53.534	71.202	1.9232	1.9232	6.257	469.25
100,000	52.190	52.228	69.852	1.902	1.9024	5.418	541.845
200,000	48.395	48.405	66.248	1.837	1.837	3.892	765.700

Thickness of pavement = 200 mm; E = 3.3 x 10^7 kN/m^2;Poisson ratio = 0.2; f_{ck} = 30 N/mm^2; f_{ctm} = 2.9 N/mm^2

Table 11 analyzes Load Case 2-interior wheel loading-at 200 mm pavement thickness. It assesses the load-bearing performance and deformation resistance of thicker pavement under centrally distributed loads.

Table 11: Load Case 2: Wheel load at the interior for pavement thickness of 200mm

Modulus of subgrade reaction ($kN/m^2/m$)	M_x(kNm/m)	M_y(kNm/m)	M_{xy} (kNm/m)	Q_x (N/mm^2)	Q_y(N/mm^2)	Maximum settlement (mm)	Base Pressure (kN/m^2)
10,000	32.775	38.3489	6.293	0.6043	0.60957	2.154	21.540
50,000	27.825	28.1469	5.8967	0.5961	0.5997	0.839	41.94
75,000	26.0571	26.0491	5.7449	0.59216	0.5957	0.697	50.906
100,000	24.722	24.6075	5.6199	0.5925	0.59258	0.586	58.620
200,000	21.366	21.2386	5.2535	0.5791	0.5829	0.415	82.98

Thickness of pavement = 200 mm; E = 3.3 x 10^7 kN/m^2; Poisson ratio = 0.2; f_{ck} = 30 N/mm^2; f_{ctm} = 2.9 N/mm^2

Table 12 summarizes the behavior of the pavement system under Load Case 3-edge wheel loading-for 200 mm thickness. It identifies the interaction between edge loading effects and pavement structural rigidity at increased depth.

International Journal of Engineering Research & Technology (IJERT)
ISSN: 2278-0181
Vol. 14 Issue 12 , December - 2025

Table 12: Load Case 3: Wheel load at the edge for pavement thickness of 200mm

Modulus of subgrade reaction ($kN/m^2/m$)	M_x(kNm/m)	M_y(kNm/m)	M_{xy} (kNm/m)	Q_x (N/mm^2)	Q_y(N/mm^2)	Maximum settlement (mm)	Base Pressure (kN/m^2)
10,000	26.507	73.949	24.659	0.8447	1.3675	6.756	67.560
50,000	25.357	55.2127	22.2009	0.833277	1.33075	2.791	139.57
75,000	24.644	50.7535	21.332	0.8263	1.3163	2.280	0.1709
100,000	24.444	47.6257	20.652	0.8199	1.3043	1.978	197.82
200,000	23.607	40.2116	19.646	0.7985	1.26839	1.409	0.2819

Thickness of pavement = 200 mm; E = 3.3 x 10^7 kN/m^2; Poisson ratio = 0.2; f_{ck} = 30 N/mm^2; f_{ctm} = 2.9 N/mm^2

Table 13 presents a summary of the cracked pavement characteristics as a function of increasing thickness. Key crack geometry descriptors such as radial distance (r), angle (θ_0), crack length (x), and crack depth (y) are tabulated for thicknesses ranging from 25 mm to 300 mm.

Table 13: Summary of Crack pavement characteristics varying with thickness

Pavement thickness (m)	r (m)	θ^0	x(m)	y (m)
0.025	1.200	1.19	2.3997	0.0499
0.50	1.201	2.38	2.3999	0.0999
0.075	1.202	3.576	2.4007	0.1500
0.100	1.204	4.7636	2.4000	0.1999
0.125	1.2005	5.95	2.4000	0.2500
0.150	1.2093	7.13	2.3999	0.3000
0.175	1.2127	8.31	2.4000	0.3503
0.200	1.2166	9.46	2.4000	0.4000
0.225	1.2209	10.62	2.4000	0.4500
0.250	1.2258	11.77	2.4000	0.5000
0.275	1.2311	12.91	2.4000	0.5501
0.300	1.2369	14.04	2.400	0.6000

International Journal of Engineering Research & Technology (IJERT)
ISSN: 2278-0181
Vol. 14 Issue 12 , December - 2025

4.2 Discussions

Crack Formation in Rigid and Flexible Pavements

The numerical analysis provided insights into the stress distribution, deformation patterns, and crack initiation points in both rigid and flexible pavements. These findings are crucial in understanding pavement deterioration mechanisms and guiding the design of more durable road structures [4].

1. Stress and Deformation Analysis

The stress distribution in rigid pavements showed that the highest tensile stresses occurred near slab corners and edges, which are common locations for crack initiation [3]. This result aligns with previous studies on concrete pavement failures, where slab curling and shrinkage exacerbate tensile stresses at these locations [1]. For flexible pavements, stress distributions indicated that tensile stresses were more significant at the surface, particularly under dual tire loading. This condition contributes to top-down cracking, a dominant distress mechanism in asphalt pavements subjected to repeated traffic loads [5]. Figure 1 illustrates the deformation patterns under varying subgrade modulus values. Pavements constructed over weaker subgrades exhibited higher deflections, increasing susceptibility to fatigue-induced cracking [11].

2. Crack Propagation Analysis

Using fracture mechanics principles, crack propagation in both rigid and flexible pavements was simulated.

Rigid Pavements: The numerical model showed that edge and corner cracks propagated toward the slab center due to stress concentration. These results align with fracture toughness predictions for concrete pavements, confirming that tensile stress beyond a critical threshold initiates cracking [2].

Flexible Pavements: Top-down cracking was analyzed using a cohesive zone model, which demonstrated that cracks initiated at the surface due to high tensile strain and propagated downward with loading cycles. This trend has been previously observed in field studies, where micro-cracks at the pavement surface gradually develop into full-depth failures [9]. Figure 2 presents a simulated crack propagation path in asphalt pavements, consistent with findings by [6].

3. Influence of Pavement Thickness and Subgrade Stiffness

The study also examined how variations in pavement thickness and subgrade stiffness affected crack initiation and propagation:

Rigid Pavements: Increasing slab thickness reduced crack propagation rates by lowering tensile stresses at the surface. This observation aligns with previous work by [12], who noted that thicker concrete slabs exhibited improved resistance to fatigue failure.

Flexible Pavements: While increased asphalt thickness delayed crack initiation, it did not eliminate crack propagation, supporting previous experimental findings [7].

Subgrade Stiffness: Higher subgrade modulus values reduced overall pavement deflection, minimizing tensile strain and delaying crack formation, which is consistent with theoretical models presented by [13].

These results suggest that optimizing pavement thickness and subgrade properties can significantly improve crack resistance, supporting recommendations for pavement design modifications [8].

4. Comparison with Experimental and Field Data

To validate the numerical model, the results were compared with experimental studies and field observations from previous research. The trends in crack propagation and stress distributions showed a strong correlation with real-world pavement failures, particularly those documented in Nigeria [14]. The numerical predictions of crack initiation and propagation closely matched field observations, reinforcing the model's applicability for practical pavement analysis [10].

International Journal of Engineering Research & Technology (IJERT)
ISSN: 2278-0181
Vol. 14 Issue 12 , December - 2025

Key Contributions and Implications

The study provides the following key contributions to pavement engineering:

A comprehensive analysis of crack initiation and propagation mechanisms in both rigid and flexible pavements.

Integration of fracture mechanics principles for a more accurate assessment of pavement durability.

Insights into the role of pavement thickness and subgrade stiffness in crack resistance.

A validated numerical approach that aligns with field data, offering practical applications for improving pavement design.

5. CONCLUSION AND RECOMMENDATIONS

This study analyzed crack initiation and propagation mechanisms in rigid and flexible pavements using finite element modeling, integrating fracture mechanics principles to improve predictive accuracy. The results highlighted key factors influencing pavement cracking, including stress distribution, deformation patterns, and the impact of pavement thickness and subgrade stiffness.

Key Findings

Crack Initiation and Propagation

- In rigid pavements, cracks predominantly initiated at slab edges and corners due to high tensile stress concentrations, consistent with previous findings on concrete pavement failures [1][3].
- In flexible pavements, top-down cracking was identified as the primary distress mechanism, with cracks initiating at the surface and propagating downward under repeated traffic loads [5][6].
- Effect of Pavement Thickness and Subgrade Stiffness
- Increasing rigid pavement thickness significantly reduced crack propagation rates by lowering surface tensile stress [12].
- While increasing asphalt thickness delayed crack initiation, it did not prevent crack propagation, aligning with previous experimental studies [7].
- Pavements with higher subgrade stiffness exhibited reduced deflections, decreasing tensile strain and delaying crack formation [13].
- Validation with Experimental and Field Data
- The numerical results closely matched real-world observations from field studies, validating the model's applicability for pavement analysis and design improvements [9][14]

Engineering Implications

The findings provide critical insights for pavement engineers and transportation authorities:

- Optimized pavement design: Proper selection of pavement thickness and subgrade properties can enhance crack resistance, reducing maintenance costs and improving road durability.
- Predictive crack modeling: Integrating fracture mechanics in numerical simulations improves the accuracy of crack progression predictions, aiding in proactive maintenance strategies.
- Field application: The validated model offers a practical tool for assessing pavement performance, supporting better decision-making in infrastructure projects.

Future Research Directions

While this study provides valuable contributions, further research is needed to refine crack modeling approaches:

- Advanced material modeling: Incorporating viscoelastic and damage mechanics models can enhance the representation of asphalt behavior under long-term loading.
- Environmental effects: Investigating the influence of temperature fluctuations and moisture on crack propagation would provide more comprehensive pavement performance predictions.

International Journal of Engineering Research & Technology (IJERT)
ISSN: 2278-0181
Vol. 14 Issue 12 , December - 2025

- Machine learning applications: Implementing AI-based predictive models could improve crack detection and maintenance planning based on real-time data.

6. DECLARATIONS

- Author Contributions:
    - Michael O. Egbebike: Conceptualization, Formal analysis, Methodology, Writing - original draft, Writing – review & editing, Project administration, Resources, Data curation, Visualization.
    - C.A. Ezeagu: Conceptualization, Methodology, Supervision, Writing – review & editing, Data curation, Project administration.
    - C.I. Ibeabuchi: Methodology, Validation, Software, Writing – review & editing, Investigation, Visualization.
- Funding: The authors received no external funding for this research.
- Conflict of Interest: The authors declare no conflict of interest.
- Ethical Approval: Not applicable.
- Data Availability: All data used in this study are available from the corresponding author upon reasonable request.

7. REFERENCES

[1] Alyamac K.E And Ince V. R.(2005) In "A Prediction Formula For Fracture Toughness Of Concrete" 7th International Fracture Conference 19-21 October 2005 Kocaeli University Kocaeli/Turkey. pp. 215 to 222.

[2] Taherkhani, H., & Tajdini, M. (2020). Investigating the performance of cracked asphalt pavement using finite elements analysis. Civil Engineering Infrastructures Journal, 53(1), 33–51.

[3] Murthy C.R. A, Palani G.S and Iyer N.R. (2009) in the State-of-the-art review on fracture analysis of concrete structural components S¯adhan¯aVol. 34, Part 2, April 2009, pp. 345–367. © Printed in India

[4] Garber, N.J., and Hoel, L.A. (2009) "Traffic and Highway Engineering", 4th Edition. Toronto, Canada: Cengage Learning

[5] Alae, M., Haghshenas, H.F. and Zhao, Y. (2019). "Evaluation of top-down crack propagation in asphalt pavement under dual tires loading", Canadian Journal of Civil Engineering, 5, pp. 185-193.

[6] Liu, P., Chen, J., Lu, G., Wang, D., Oeser, M., & Leischner, S. (2019). Numerical simulation of crack propagation in flexible asphalt pavements based on cohesive zone model developed from asphalt mixtures. Materials, 12(8), 1278.

[7] Yang, D.; Karimi, H.R.; Aliha, M.R.M. (2021) Comparison of Testing Method Effects on Cracking Resistance of Asphalt Concrete Mixtures. Applied Sciences, 11(11), 5094.

[8] Sun,L., Wang, G., Zhang, H. and Liu, L. (2018)Initiation and Propagation of Top-Down Cracking in Asphalt Pavement, Applied Sciences, 8, 774. https://doi:10. 3390/app8050774

[9] Wu, S., Wen, H., Zhang, W., Shen, S., Mohammad, L. N., Faheem, A. and Muhunthan, B. (2019). Field performance of top-down fatigue cracking for warm mix asphalt pavements, International Journal of Pavement Engineering, 20(1), pp. 33-43

[10] Ezeagu, C.A, Udebunu, J.N and Obiorah S. M.O, (2015) " Destructive and Non-Destructive Assessment of Collapsed Structures in Onitsha, Anambra State, Nigeria" American Scientific Research Journal for Engineering, Technology, and Sciences (ASRJETS) © Global Society of Scientific Research and Researchers. http://asrjetsjournal.org/ Vol. 12 No 1. May. Pp170-187.

[11] Ezeagu, C.A., Ibeabuchi, C.I. and Mezie, E.O. (2020) "Empirical Post-mortem analysis and healing approach of flexible and rigid pavement failures in Anambra state" Journal of Inventive Engineering and Technology (JIET) Vol. 1, Issue 2, January, pp. 42-53.

[12] Oguara T.M. (2006), Highway Engineering Pavement Design, Construction and Maintenance Malthouse press limited.

[13] Ogbezobe J, Adeleke I.A, and Adebayo A.(2018)"Influence of Compressive, Tensile and Fatigue Stresses on Asphalt and Concrete Cement Road Pavements in Nigeria - Using Linear Elastic Theory" July, Journal of Engineering Research and Reports

[14] Ezeagu C.A. (2018), "Controlling Building and Infrastructure Collapse in Nigeria" - A guest speaker lecture presented at workshop organized by SON on "General Sensitization For Increase Awareness on Building Collapse" at Nelrose Hotels Asaba pg 1-17 March.